Multi-Agent Deep Reinforcement Learning for Energy Efficient Multi-Hop STAR-RIS-Assisted Transmissions

Pei-Hsiang Liao, Li-Hsiang Shen*, Po-Chen Wu, and Kai-Ten Feng
Department of Electronics and Electrical Engineering, National Yang Ming Chiao Tung University, Hsinchu, Taiwan
*Department of Communication Engineering, National Central University, Taoyuan, Taiwan
Email: phliao.ee11@nycu.edu.tw, shen@ncu.edu.tw, wupochen.ee11@nycu.edu.tw, and ktfeng@nycu.edu.tw

Abstract—Simultaneously transmitting and reflecting reconfigurable intelligent surface (STAR-RIS) provides a promising way to expand coverage in wireless communications. However, limitation of single STAR-RIS inspire us to integrate the concept of multi-hop transmissions, as focused on RIS in existing research. Therefore, we propose the novel architecture of multi-hop STAR-RISs to achieve a wider range of full-plane service coverage. In this paper, we intend to solve active beamforming of the base station and passive beamforming of STAR-RISs, aiming for maximizing the energy efficiency constrained by hardware limitation of STAR-RISs. Furthermore, we investigate the impact of the on-off state of STAR-RIS elements on energy efficiency. To tackle the complex problem, a Multi-Agent Global and locAl deep Reinforcement learning (MAGAR) algorithm is designed. The global agent elevates the collaboration among local agents, which focus on individual learning. In numerical results, we observe the significant improvement of MAGAR compared to the other benchmarks, including Q-learning, multi-agent deep Q network (DQN) with golbal reward, and multi-agent DQN with local rewards. Moreover, the proposed architecture of multi-hop STAR-RISs achieves the highest energy efficiency compared to mode switching based STAR-RISs, conventional RISs and deployment without RISs or STAR-RISs.

Index Terms—STAR-RIS, multi-agent, deep reinforcement learning, energy efficiency.

I. INTRODUCTION

Reconfigurable intelligent surfaces (RISs) have emerged as a promising technology to improve the capacity and reliability of wireless communication [1]. By controlling and manipulating configurations of RIS elements, a virtual line-of-sight (LoS) link is created to bypass obstacles between transceivers [2]. Leveraging these significant benefits, study [3] aims to maximize the downlink transmission rate. Consequently, RIS technology enables the achievement of targeted signal distributions, leading to significant improvements in communication performance [4]. However, limited by only reflecting signals, RIS cannot be fully utilized when the transmitters and receivers are located on opposite sides.

As a remedy, simultaneously transmitting and reflecting RIS (STAR-RIS) enables 360° full-plane coverage. In contrast to

¹This work was supported in part by the National Science and Technology Council (NSTC) under Grant NSTC 113-2221-E-A49-119-MY3, Grant 113-2218-E-A49-026, Grant 113-2218-E-A49-027, Grant 112UC2N006, Grant 112UA10019; in part by the Higher Education Sprout Project of the National Yang Ming Chiao Tung University (NYCU) and Ministry of Education (MoE); in part by the Co-creation Platform of the Industry-Academia Innovation School, NYCU, under the framework of the National Key Fields Industry-University Cooperation and Skilled Personnel Training Act, from the MOE and industry partners in Taiwan, and in part by the Hon Hai Research Institute, Taipei, Taiwan.

traditional RIS, the STAR-RIS eliminates deployment restrictions to specific geographic areas. A growing body of research investigates the use of STAR-RIS to enhance communication systems [5], [6]. In [5], the authors analyze the energy efficiency of the system with optimization of the beamforming of BS and the configuration of STAR-RIS. In addition, the authors of [6] integrate the mode switching design in STAR-RIS to maximize the achievable sum-rate. Although research into STAR-RIS intensifies, the potential of cooperative multiple STAR-RISs is emerging as an alternative approach to enhance coverage.

Since multiple distributed RISs without signal cooperation uniquely reflects the signals to users, the concept of multi-hop transmissions has been proposed to enlarge the coverage and connectivity. Furthermore, multi-hop reflections are established through inter-RIS links, and provide blockage-free links with higher transmission quality [7], [8]. The authors of [7] propose a machine learning-based approach to optimize RIS beamforming. In [8], the authors design the beamforming of BS and RISs by leveraging deep learning. However, existing research has primarily focused on multi-hop RIS systems. Inspired by these approaches, we propose the novel architecture of multi-hop STAR-RISs, enabling a wider range of full-plane service coverage.

In this paper, we present a multi-hop communications assisted by STAR-RISs to overcome the propagation attenuations and improve the coverage range. In particular, we consider the on-off state of STAR-RIS elements, which is not considered in most of existing papers. However, traditional algorithms possess high complexity to find solutions with large coefficients. Deep reinforcement learning (DRL) is especially suitable for unknown environments without channel estimation [9]–[11]. To achieve long-term performance benefits in a multi-hop STAR-RIS system, we design a DRL-enhanced algorithm to optimize joint active BS and passive STAR-RIS beamforming. The contributions of this work are summarized as follows.

- We consider multi-hop STAR-RISs with joint optimization
 of active BS and passive STAR-RIS beamforming for
 maximizing the system energy efficiency. Additionally, we
 investigate the on-off mechanism of STAR-RIS elements to
 address the potential of high power consumption of STARRISs.
- We have proposed a Multi-Agent Global and locAl deep Reinforcement learning (MAGAR) algorithm with collaborative multiple agents. Local agents perform local learning and facilitate independent interaction with the environment.

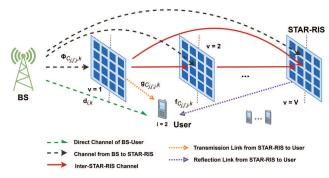


Fig. 1: System architecture of the proposed multi-hop STAR-RIS

In contrast, the global agent periodically replaces local agents to dictate actions, thereby optimizing the overall system performance.

Benefiting from the global-local agent design, MAGAR achieves the highest energy efficiency among the other benchmarks of multi-agent deep Q network (DQN) and conventional Q-learning. Moreover, the multi-hop STAR-RISs have achieved higher performance than the mode switching based STAR-RISs, conventional RISs, and deployment without RISs/STAR-RISs.

II. SYSTEM MODEL AND PROBLEM FORMULATION

A. System Model

As depicted in Fig. 1, we consider a single BS serving K_i user equipments (UEs) per region, with I total regions. Note that all users are equipped with a single antenna. The V STAR-RIS placed to enhance signal propagation and potentially enhance service coverage. The respective sets of STAR-RISs, service region and users are defined as $\mathcal{V} = \{1, ..., V\}$, $\mathcal{I} = \{1, ..., I\}$ and $\mathcal{K}_i = \{1, ..., K_i\}$. The propagation of signals is also delineated in Fig. 1, illustrating all conceivable signal pathways, assuming a user is located in 2-th region. We define $\mathcal{C} = \{\mathcal{C}_i, \forall j \in \mathcal{V}\}$ as the set corresponding to all possible paths, where j indicates the number of STAR-RISs which the signal experiences through. Furthermore, $C_j = \{\mathbf{C}_{j,j'}, \forall j' \in |C_j'|\}$ is the set of all possible paths with j STAR-RISs, where the tuple $\mathbf{C}_{j,j'} = (C_{j,j',1},...,C_{j,j',j})$ corresponding to the signal passing through j STAR-RISs. In each item, the first subscript of each item j is the number of signal passing through, the second subscript j' is the index of possible permutations of the set C_i' in lexicographic order, and the third subscript is the index of the permutation. Moreover, we assume that the orientations of all STAR-RISs face forward the BS. Note that the property of each item in $C_{j,j'}$ represents the index of STAR-RIS will be arranged in ascending order.

B. STAR-RIS

The BS is equipped with a uniform linear array comprising Mtransmit antennas and the STAR-RISs we employed are energy splitting (ES) [12]. We define N_v as the number of elements of the v-th STAR-RIS. For analysis convenience, we consider $N_v = N, \forall v \in \mathcal{V}$ with a set of $\mathcal{N} = \{1, \dots, N\}$. Furthermore, we denote the set $\mathcal{U} = \{\mathcal{R}, \mathcal{T}\}$ as the reflection and transmission

functionality set, respectively. For the v-th STAR-RIS, the onoff matrix Λ_v and the passive beamforming matrix Ξ_v^u having diagonal structures are denoted as

$$\mathbf{\Lambda}_{v} = \operatorname{diag}\left(\alpha_{v,1}, \dots, \alpha_{v,n}, \dots, \alpha_{v,N}\right), \quad \forall v \in \mathcal{V}, \tag{1a}$$

$$\mathbf{\Xi}_{v}^{u} = \operatorname{diag}\left(\beta_{v,1}^{u} e^{j\theta_{v,1}^{u}}, \dots, \beta_{v,n}^{u} e^{j\theta_{v,n}^{u}}, \dots, \beta_{v,N}^{u} e^{j\theta_{v,N}^{u}}\right),$$

$$\forall v \in \mathcal{V}, u \in \mathcal{U}, \tag{1b}$$

$$\mathbf{\Theta}_{v}^{u} = \mathbf{\Lambda}_{v} \mathbf{\Xi}_{v}^{u}, \qquad \forall v \in \mathcal{V}, u \in \mathcal{U}, \tag{1c}$$

where $\alpha_{v,n} \in \{0,1\}$ stands for whether the *n*-th element of STAR-RIS is selected to be switched on. The notations of $\beta^u_{v,n} \in [0,1]$ and $\theta^u_{v,n} \in [0,2\pi)$ represent the amplitude and phase shift of the n-th element of STAR-RIS, respectively. We represent the set of on-off as $\Lambda = \{\Lambda_v, \forall v \in \mathcal{V}\}$ and passive beamforming $\Xi = \{\Xi_v^u, \forall v \in \mathcal{V}, u \in \mathcal{U}\}$. Furthermore, due to limitations imposed by the electric and magnetic impedance, the energy conservation constraint and the coupling effect between the reflected and transmitted phase shifts [13] is obtained as

$$\beta_{v,n}^{\mathcal{T}} = \sqrt{1 - \left(\beta_{v,n}^{\mathcal{R}}\right)^2}, \qquad \forall v \in \mathcal{V}, n \in \mathcal{N}, \qquad \text{(2a)}$$

$$\theta_{v,n}^{\mathcal{T}} = \theta_{v,n}^{\mathcal{R}} \pm \frac{\pi}{2}, \qquad \forall v \in \mathcal{V}, n \in \mathcal{N}. \qquad \text{(2b)}$$

$$\theta_{v,n}^{\mathcal{T}} = \theta_{v,n}^{\mathcal{R}} \pm \frac{\pi}{2}, \qquad \forall v \in \mathcal{V}, n \in \mathcal{N}.$$
 (2b)

C. Channel Model

For the k-th user in the region i, we denote $\mathbf{d}_{i,k} \in \mathbb{C}^{M \times 1}$, $\mathbf{g}_{C_{j,j',j},k} \in \mathbb{C}^{N \times 1}$, and $\mathbf{f}_{C_{j,j',j},k} \in \mathbb{C}^{N \times 1}$ as direct channels from the BS to the user, transmitted channels, and reflected channels from the $C_{j,j',j}$ -th STAR-RIS to the user, respectively. The channels from the BS to the $C_{j,j',1}$ -th STAR-RIS is denoted as $\Phi_{C_{j,j'},1} \in \mathbb{C}^{M \times N}$ and channels from the $C_{j,j',l}$ -th to the $C_{j,j',l+1}$ -th STAR-RISs are denoted as $\Phi_{C_{j,j'},l}$ - $C_{j,j',l+1} \in \mathbb{C}^{N \times N}$. We assume that the channels associated with the BS and STAR-RISs is indicated by $\mathbf{H} \in \mathbb{C}^{N \times N}$. $\left\{\mathbf{d}_{i,k},\mathbf{g}_{C_{j,j',j},k},\mathbf{f}_{C_{j,j',j},k},\Phi_{C_{j,j',l},C_{j,j',l+1}}\right\} \ \text{obeys the Rician distribution which is given by}$

$$\mathbf{H} = \frac{1}{\sqrt{\rho}} \left(\sqrt{\frac{\mathcal{K}}{\mathcal{K} + 1}} \mathcal{L}_{LoS} + \sqrt{\frac{1}{\mathcal{K} + 1}} \mathcal{L}_{NLoS} \right), \quad (3)$$

where K is the Rician factor, and \mathcal{L}_{LoS} and \mathcal{L}_{NLoS} are denoted as the LoS and NLoS components, respectively. The symbol ρ refers to as the distance-based pathloss expressed as [14] $PL(dB) = 10 \log_{10} \rho = 32.4 + 20 \log_{10} \omega + 21 \log_{10} \varsigma$, where ω represents the central operating frequency and ς denotes the distance between the transmitter and receiver. Thereby, the effective STAR-RIS channel $\Omega_{i,k}$ between the BS and k-th user in i-th region can be formulated as

$$\Omega_{i,k} = \mathbf{d}_{i,k}^{\mathcal{H}}
+ \sum_{j \in \mathcal{V}} \sum_{j' \in \mathcal{C}_{j}'} \left(\mathbb{1}_{\left\{C_{j,j',j} < i\right\}} \cdot \mathbf{g}_{C_{j,j',j},k}^{\mathcal{H}} \mathbf{\Theta}_{C_{j,j',j}}^{\mathcal{T}} f_{\prod} \left(\mathbf{C}_{j,j'}\right) \right)
+ \mathbb{1}_{\left\{C_{j,j',j} \ge i\right\}} \cdot \mathbf{f}_{C_{j,j',j},k}^{\mathcal{H}} \mathbf{\Theta}_{C_{j,j',j}}^{\mathcal{R}} f_{\prod} \left(\mathbf{C}_{j,j'}\right) \right), \quad (4a)$$

$$f_{\prod} \left(\mathbf{C}_{j,j'}\right) = \prod_{l=1}^{j-1} \left(\mathbf{\Phi}_{C_{j,j',l},C_{j,j',l+1}} \mathbf{\Theta}_{C_{j,j',l}}^{\mathcal{T}}\right) \mathbf{\Phi}_{C_{j,j',1}}, \quad (4b)$$

where 1 denotes the indicator function representing the event occurrence and \mathcal{H} represents the hermitian of a matrix. The function 1 takes a value of 1 when the event occurs and

0 otherwise. In (4a), apart from $\mathbf{d}_{i,k}^{\mathcal{H}}$ represented as the direct link, the other links are categorized into transmitted links of $\mathbf{g}_{C_{j,j',j},k}^{\mathcal{H}} \Theta_{C_{j,j',j}}^{\mathcal{T}} f_{\prod}(\mathbf{C}_{j,j'})$ and reflected links of $\mathbf{f}_{C_{j,j',j},k}^{\mathcal{H}} \Theta_{C_{j,j',j}}^{\mathcal{R}} f_{\prod}(\mathbf{C}_{j,j'})$ based on a comparison of the indices of STAR-RISs $C_{j,j',j}$ and region i. The product $f_{\prod}(\mathbf{C}_{j,j'})$ in (4b) can be used to calculate the cascaded STAR-RIS channel.

D. Signal Model

The transmitted signal and the active beamforming vector of the k-th user in the i-th region are defined as $x_{i,k} \in \mathbb{C}^{1 \times 1}$ and $\mathbf{w}_{i,k} \in \mathbb{C}^{M \times 1}$, respectively. In consequence, the received signal of the k-th user in the i-th region is given by

$$y_{i,k} = \mathbf{\Omega}_{i,k} \sum_{i' \in \mathcal{I}} \sum_{k' \in \mathcal{K}_i} \mathbf{w}_{i',k'} x_{i',k'} + n_{i,k}, \tag{5}$$

where $n_{i,k}$ is Gaussian noise. As known in (4) and (5), the corresponding SINR is given by

$$\Gamma_{i,k} =$$

$$\frac{\left|\mathbf{\Omega}_{i,k}\mathbf{w}_{i,k}\right|^{2}}{\sum_{k'\in\tilde{\mathcal{K}}_{i}}\left|\mathbf{\Omega}_{i,k}\mathbf{w}_{i,k'}\right|^{2}+\sum_{i'\in\tilde{\mathcal{I}}}\sum_{k'\in\mathcal{K}_{i'}}\left|\mathbf{\Omega}_{i,k}\mathbf{w}_{i',k'}\right|^{2}+\sigma^{2}},$$
(6)

where $\tilde{\mathcal{K}}_i = \{\mathcal{K}_i \setminus k\}$ and $\tilde{\mathcal{I}} = \{\mathcal{I} \setminus i\}$. The first term in the denominator is the interference from users within the same region i, the second term is from users in the other regions, and σ^2 represents the noise power. According to (6), the data rate of the system can be calculated as

$$R = \sum_{i \in \mathcal{I}} \sum_{k \in \mathcal{K}_i} B \log_2 \left(1 + \Gamma_{i,k} \right), \tag{7}$$

where B represents the bandwidth.

Moreover, we denote the set of active beamforming as $\mathbf{W} = \{\mathbf{W}_i, \forall i \in \mathcal{I}\}$ with the beamforming matrix of the *i*-region $\mathbf{W}_i = [\mathbf{w}_{i,1}, ..., \mathbf{w}_{i,K_i}]$. Consequently, the power constraint for the BS is expressed as

$$\sum_{i \in \mathcal{I}} \operatorname{tr} \left\{ \mathbf{W}_i \mathbf{W}_i^{\mathcal{H}} \right\} \le P_{\max}, \tag{8}$$

where tr $\{\cdot\}$ denotes the trace operation of the matrix and P_{max} is the transmit power budget for the BS. Moreover, the power of the n-th element of the v-th STAR-RIS is given by

$$\gamma_{v,n} = p \cdot \alpha_{v,n}, \ \forall v \in \mathcal{V}, n \in \mathcal{N},$$
 (9)

where the constant p represents the power consumed by each element of STAR-RISs. The total power consumption of the entire system is calculated as

$$P_{total} = \sum_{v \in \mathcal{V}} \sum_{n \in \mathcal{N}} \gamma_{v,n} + \sum_{i \in \mathcal{I}} \operatorname{tr} \left\{ \mathbf{W}_{i} \mathbf{W}_{i}^{\mathcal{H}} \right\}. \tag{10}$$

Therefore, the total energy efficiency is given by

$$E\left(\mathbf{\Lambda}, \mathbf{\Xi}, \mathbf{W}\right) = \frac{R}{P_{total}},\tag{11}$$

with the variables Λ , Ξ , and W.

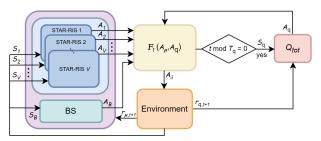


Fig. 2: Proposed MAGAR algorithm.

E. Problem Formulation

The objective is to maximize the energy efficiency while guaranteeing the constraints of the STAR-RIS. The corresponding optimization problem is formulated as

$$\max_{\mathbf{\Lambda}, \mathbf{\Xi}, \mathbf{W}} E(\mathbf{\Lambda}, \mathbf{\Xi}, \mathbf{W}), \qquad (12a)$$

s.t.
$$\sum_{i \in \mathcal{I}} \operatorname{tr} \left\{ \mathbf{W}_i \mathbf{W}_i^{\mathcal{H}} \right\} \le P_{\max}, \tag{12b}$$

$$\beta_{v,n}^{\mathcal{T}} = \sqrt{1 - (\beta_{v,n}^{\mathcal{R}})^2}, \quad \forall v \in \mathcal{V}, n \in \mathcal{N}, \quad (12c)$$

$$\theta_{v,n}^{\mathcal{T}} = \theta_{v,n}^{\mathcal{R}} \pm \frac{\pi}{2}, \quad \forall v \in \mathcal{V}, n \in \mathcal{N},$$
 (12d)

$$\alpha_{v,n} \in \{0,1\}, \quad \forall v \in \mathcal{V}, n \in \mathcal{N},$$
 (12e)

$$0 \le \beta_{v,n}^u \le 1, \quad \forall v \in \mathcal{V}, n \in \mathcal{N}, u \in \mathcal{U}, \quad (12f)$$

$$0 \le \theta_{v,n}^u \le 2\pi, \quad \forall v \in \mathcal{V}, n \in \mathcal{N}, u \in \mathcal{U}.$$
 (12g)

Constraint (12b) is the maximum transmit power constraint of the BS. Constraints on amplitude in (12c) and phase shift in (12d) describe the coupling relationship between transmission and reflection capability of STAR-RISs. Constraints (12e), (12f) and (12g) characterize the binary on-off state and limitations of the amplitude and phase shift of STAR-RISs. Problem (12) presents an obstacle due to its non-convex and non-linear nature with fractional functions and logarithmic expressions. Therefore, we propose a DRL-based algorithm to deal with the above problems, which is elaborated in the following section.

III. PROPOSED MAGAR ALGORITHM

However, a centralized solution employing a single-agent RL with large and complex observation spaces lead to insufficient memory storage and slow convergence. As a remedy, the multiagent DRL (MA-DRL) algorithm enable each agent to operate independently, improving flexibility and efficiency in handling complex scenarios. However, training the independent agents for optimizing the team reward presents a challenge. Motivated by these challenges, we propose MAGAR solves the complex problem (12) by exchanging the execution of global and local agents. MAGAR not only effectively optimizes the global reward, but also enhances cooperation among local agents.

A. Markov Decision Process

By reformulating (12) as a Markov decision process (MDP), our objective is to maximize the accumulated reward (11) $\mathbb{E}[\sum_{t=1}^{T} \gamma^t r_{t+1}]$, where $\gamma \in [0,1]$ denotes the discount factor, r_{t+1} is the reward function and T is the end time slot of an episode. We define all STAR-RISs and BS as agents with

their own MDP $(S_{\mu,t}, A_{\mu,t}, P_{\mu,t}, r_{\mu,t+1})$, $\forall \mu \in \{v, \mathcal{B}, \forall v \in \mathcal{V}\}$ and \mathcal{B} represents the agent of the BS. Moreover, we define $(S_{\mathbf{q},t}, \mathcal{A}_{\mathbf{q},t}, P_{\mathbf{q},t}, r_{\mathbf{q},t+1})$ as the MDP of the global agent Q_{tot} , where the reward $r_{\mathbf{q},t}$ is shared among the whole system. In the following, we simplify the sets of states and actions $S_{\mu,t}$, $S_{\mathbf{q},t}$, $A_{\mu,t}$, and $A_{\mathbf{q},t}$ as S_{μ} , $S_{\mathbf{q}}$, A_{μ} , and $A_{\mathbf{q}}$, respectively.

B. Proposed MAGAR Algorithm

As depicted in Fig. 2, our proposed MAGAR algorithm comprises two components. The first component involves independent training for each agent to interact with the environment and receives an agent-specific reward $r_{\mu,t}$. This promotes individual exploration where agents may converge to the suboptimal actions due to limited observation. The second component emphasizes global optimization of the entire system by a global agent denoted as Q_{tot} . Two different actions \mathcal{A}_{μ} for each agent and \mathcal{A}_{q} for the global agent will be performed based on

$$F_t(\mathcal{A}_{\mu}, \mathcal{A}_{\mathbf{q}}) = \begin{cases} \mathcal{A}_{\mathbf{q}}, & \text{if } t \text{ mod } T_{\mathbf{q}} = 0, \\ \mathcal{A}_{\mu}, & \text{otherwise,} \end{cases}$$
 (13)

where $T_{\rm q}>0$ represents the execution period by the global agent. With comprehensive information gathered from all agents within the global state $\mathcal{S}_{\rm q}$, the global agent is empowered to make better decisions $\mathcal{A}_{\rm q}$. Although Q_{tot} can acquire complete state information from all agents, frequent execution of the global agent leads to computational overhead. Therefore, the periodic nature of the replacement by Q_{tot} strikes a balance between achieving global optimization and avoiding burdening the system.

- State: For each STAR-RIS agent, we denote $S_v = \{\beta_{v,n}^{\mathcal{R}}, \theta_{v,n}^{\mathcal{R}}, \theta_{v,n}^{\mathcal{T}}, \alpha_{v,n}, \forall n \in \mathcal{N}\}$ as the state of the v-th STAR-RIS, comprising the amplitude of part \mathcal{R} , phase shifts of both parts \mathcal{R} and \mathcal{T} , as well as on-off state. For the BS agent, we decompose the beamforming matrix into real and imaginary parts, as the state of $S_{\mathcal{B}} = \{\mathbf{W}^{\zeta}, \mathbf{W}^{\eta}\}$, where ζ and η are the real and imaginary operation. For the global agent, we denote $S_{\mathbf{q}} = \{S_v, S_{\mathcal{B}}, \forall v \in \mathcal{V}\}$.
- Action: For each STAR-RIS agent, we define the action set which includes increment/decrement of amplitude and phase shifts, as well as on-off policy as $\mathcal{A}_v = \left\{\pm \Delta_{\beta_{v,n}^{\mathcal{R}}}, \pm \Delta_{\theta_{v,n}^{\mathcal{R}}}, \vartheta_{v,n}, \alpha_{v,n}, \forall v \in \mathcal{V}, n \in \mathcal{N}\right\}$, where ϑ_n determines the phase difference between $+\frac{\pi}{2}$ and $-\frac{\pi}{2}$ as well as $\alpha_n \in \{0,1\}$. Here, $\Delta_{\beta_{v,n}^{\mathcal{R}}} > 0$ and $\Delta_{\theta_{v,n}^{\mathcal{R}}} > 0$ represent redefined step sizes for $\beta_{v,n}^{\mathcal{R}}$ and $\theta_{v,n}^{\mathcal{R}}$ within the intervals [0,1] and $[0,2\pi)$, respectively. For the BS agent, we define the set of actions for increment/decrement of the real and imaginary parts of the beamforming matrix as $\mathcal{A}_{\mathcal{B}} = \{\pm \Delta_{\zeta}, \pm \Delta_{\eta}\}$, where $\Delta_{\zeta} > 0$ and $\Delta_{\eta} > 0$ represent the step size of each BS's antenna. For the global agent, we denote $\mathcal{A}_{\mathbf{q}} = \{\mathcal{A}_{v}, \mathcal{A}_{\mathcal{B}}, \forall v \in \mathcal{V}\}$.

We denote $s_{\delta,t} \in \mathcal{S}_{\delta}$ and $a_{\delta,t} \in \mathcal{A}_{\delta}$ as the input and output of the environment. At the t-th time slot, an agent select an action $a_{\delta,t} \in \mathcal{A}_{\delta}$ based on the ϵ -greedy policy as

$$a_{\delta,t} = \begin{cases} \text{Randomly select from } \mathcal{A}_{\delta}, & \text{if } rand() \leq \epsilon, \\ \operatorname{argmax}_{a_{\delta,t}} Q\left(s_{\delta,t}, a_{\delta,t}\right), & \text{otherwise,} \end{cases}$$
(14)

with the exploration probability defined as ϵ , the state as $s_{\delta,t} \in \mathcal{S}_{\delta}$, and the $Q\left(s_{\delta,t},a_{\delta,t}\right)$ as action-value function. The next state will be updated as $s_{\delta,t+1} \leftarrow s_{\delta,t} + a_{\delta,t}$ if the value is within the legitimate state space. Otherwise, the next state will remain unchanged as $s_{\delta,t+1} \leftarrow s_{\delta,t}$. Furthermore, to satisfy the constraint (12b), we normalize the beamforming matrix by $\sum_{i\in\mathcal{I}} \operatorname{tr}\left\{\mathbf{W}_i\mathbf{W}_i^{\mathcal{H}}\right\} = P_{\max}$. With the constraint of STAR-RIS (12f), $\beta_{v,n}^{\mathcal{T}}$ and Θ_v^u could be obtained. Therefore, at t-th time slot, the updated state of each agent is employed to compute the individual reward $R_{\mu,t}$ and power consumption $P_{\mu,t}$. In particular, except the states of agent i all agents remain unaltered during the calculation of $R_{\mu,t}$.

Moreover, we define the global reward function as

$$r_{\mathbf{q},t} = \frac{R_t}{P_{total,t}},\tag{15}$$

where R_t and $P_{total,t}$ represent the achievable rate and the total power consumption obtained at t-th time slot. However, as observed in [15], MA-RL may have the issue of partial local observability. A few agents learn a beneficial policy, while the other agents intend to act lazily during learning owing to the shared global reward. Accordingly, we introduce an additional reward function for each agent as

$$r_{\mu,t} = \frac{R_{\mu,t}}{P_{\mu,t}}. (16)$$

The optimal target value for each agent is indicated as $y_{\mu} = r_{\mu,t+1} + \gamma \max_{a_{\mu}} Q_{\mu,t} (s_{\mu,t+1}, a_{\mu})$. Therefore, agents learn their optimal policies through refining the individual Q-value function, which can be represented by

$$Q_{n+1}(s_{n+1}, a_{n+1}) \leftarrow (1-\lambda)Q_{n+1}(s_{n+1}, a_{n+1}) + \lambda y_n.$$
 (17)

Here, λ denotes the learning rate. The notation $r_{\mu,t+1}$ is the immediate reward obtained by executing the action $a_{\mu,t} \in \{\mathcal{A}_v, \mathcal{A}_{\mathcal{B}}\}$, $\forall v \in \mathcal{V}$ in the state $s_{\mu,t} \in \{\mathcal{S}_v, \mathcal{S}_{\mathcal{B}}\}$, $\forall v \in \mathcal{V}$ at the t-th time slot. We employ a neural network function approximator with weights ξ as a Q-network. Otherwise, for each agent, we define $\psi_{\mu} = r_{\mu,t+1} + \gamma \max_{a_{\mu}} Q_{\mu,t} \left(s_{\mu,t+1}, a_{\mu}; \xi_{\mu,\tau}^{-}\right)$, where $\xi_{\mu,\tau}^{-}$ denotes the Q-network parameters from some previous time slots. Consequently, the loss function can be given by

$$L_{\mu}(\xi_{\mu,\tau}) = \mathbb{E}\left[\left(\psi_{\mu} - Q_{\mu,t} \left(s_{\mu,t}, a_{\mu,t}; \xi_{\mu,\tau} \right) \right)^{2} \right], \tag{18}$$

where $\xi_{\mu,\tau}$ represent the parameter at τ iteration of the current network for each agent.

However, limited observation potentially leading to the local optimum. To address this issue, we propose a cooperative multi-agent architecture to facilitate information exchange and coordination among agents. The complete information $s_{\mathbf{q},t} \in \mathcal{S}_{\mathbf{q}} = \mathcal{S}_v \cup \mathcal{S}_{\mathcal{B}}$ is aggregated from each individual agent. Then, the global agent determines a joint action $a_{\mathbf{q},t} \in \mathcal{A}_{\mathbf{q}} = \mathcal{A}_v \cup \mathcal{A}_{\mathcal{B}}$ from each agent. Moreover, we determine $\max_{a_{\mu}} Q_{\mu,t} \left(s_{\mu,t}, a_{\mu} \right)$ as the maximum Q value obtained from each agent in the previous time slot. For the global agent, we define the optimal target value as $y_{\mathbf{q}} = r_{\mathbf{q},t+1} + \gamma \sum_{\mu} \max_{a_{\mu}} Q_{\mu,t} \left(s_{\mu,t}, a_{\mu} \right)$, which incorporates the immediate reward $r_{\mathbf{q},t+1}$ predefined in (15). Specifically, summarizing the maximum Q values from local agents elevates the cooperation of the entire system. Therefore, we approximate the optimal action-value function of global

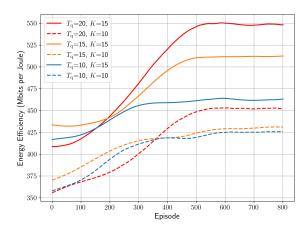


Fig. 3: Convergence behavior of the proposed MAGAR algorithm.

agent by $Q_{q,t+1}$ $(s_{\mathbf{q},t},a_{\mathbf{q},t})$, which is analogous to (17) but with subscript μ replaced by \mathbf{q} . To train the global Q-network, we employ the parameters $\xi_{\mathbf{q},\tau}^-$ from the previous time slots, where the optimal target values $y_{\mathbf{q}}$ are substituted with approximate target values $\psi_{\mathbf{q}} = r_{\mathbf{q},t+1} + \gamma \sum_{\mu} \max_{a_{\mu}} Q_{\mu,t} \left(s_{\mu,t},a_{\mu};\xi_{\mathbf{q},\tau}^-\right)$. This leads to a sequence of the loss function of Q_{tot} , $L_{\mathbf{q}}(\xi_{\mathbf{q},\tau})$, which is achieved by substituting the subscript symbol μ in (18) with \mathbf{q} .

IV. PERFORMANCE EVALUATION

In this section, the results of the simulations are presented to evaluate the performance of the proposed MAGAR algorithm in multi-hop STAR-RIS system, serving total users $K = \sum_{i \in \mathcal{I}} K_i$. The transmit power of the BS is set to 33 dBm, whilst the power of each STAR-RIS element is set to p=17 dBm. The noise power is $\sigma^2 = -174 + 10 \log_{10} B$ dBm, where B=100 MHz is the operating bandwidth. The carrier frequency is set to $\omega=28$ GHz. In our MAGAR algorithm, the simulation parameters are as $\{T_{\rm cl}, \epsilon, \lambda, \gamma\} = \{20, 0.3, 0.1, 0.9\}$.

In Fig. 3, we investigate the convergence of MAGAR across varying numbers of users, considering $M=5,\ V=3,\ N=16,\ \varsigma=10.$ We observe that the frequency of the global optimization agent Q_{tot} plays a crucial role in influencing reward performance. Infrequent execution fosters autonomous exploration by agents, potentially leading to effective reward optimization, while excessive execution of Q_{tot} can introduce overhead and hinder reward acquisition. Moreover, the simulation results demonstrate a positive correlation between the number of users served by the system and the reward.

In Fig. 4, we evaluate the performance of MAGAR under different numbers of STAR-RIS elements N, and number of STAR-RISs V. We consider $T_{\rm q}=20,\ M=5,\ K=10,$ and $\varsigma=10.$ Also, we investigate the performance of three on-off policies, **all-on**: all elements are switched on, **half-on**: randomly switch on half elements of the STAR-RISs, **optimized**: dynamically and optimally selected by MAGAR. We observe that the trend in energy efficiency exhibits an initial ascent followed by a subsequent decline. As the number of elements continues to grow, the dominance of power consumption outweighs the gains in the sum rate, ultimately leading to a deterioration of energy efficiency. The results demonstrate that the optimized on-off

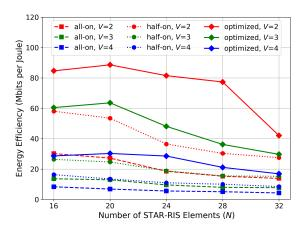


Fig. 4: The energy efficiency performance versus different numbers of N and V under different operating mechanism of all-on, half-on, and optimized.

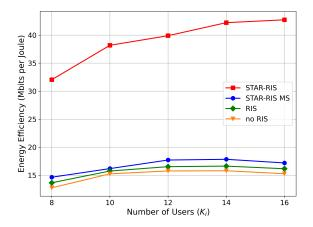


Fig. 5: The energy efficiency of the system assisted by multi-hop STAR-RIS, STAR-RIS MS, RIS, and deployment without RIS.

mechanism outperforms the other two cases. Specifically, the configurations in which all elements are operational exhibit the worst performance, owing to the associated high power cost.

In Fig. 5, we study the impact of users within the multihop STAR-RIS-aided system across various operational modes, including the ES mode, mode switching (MS) based STAR-RISs [12], conventional RISs, and the scenario without RISs. We consider $T_{\rm q}=20,\ M=5,\ V=2,\ N=16,$ and $\varsigma=10.$ We can observe that the augmenting of serving users correlates with increasings energy efficiency. In contrast to conventional RISs, STAR-RIS offers superior performance. Furthermore, the proposed ES-based multi-hop STAR-RISs demonstrate the highest EE performance. This is attributed to the amplitude control capabilities of all the STAR-RIS elements, which facilitate superior interference management compared to the fixed amplitude in MS mode. In contrast, transmission without RIS only provides direct link channels, resulting in inferior performance.

The impact of STAR-RIS deployment is analyzed in Fig. 6, with $T_{\rm q}=20,\ M=5,\ V=2,\ N=16,$ and K=10. We consider the deployment of the STAR-RIS is along the x-axis with an inter STAR-RIS distance of ς , where the first element is placed at $(0,\varsigma)$. Users are randomly distributed in

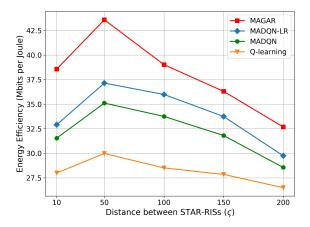


Fig. 6: Comparison of proposed MAGAR algorithm and benchmarks versus the various distance between STAR-RISs ς .

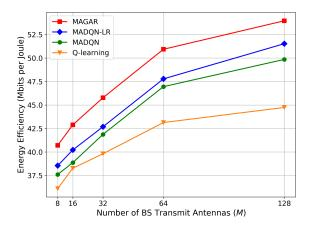


Fig. 7: The energy efficiency of MAGAR and benchmarks versus different numbers of BS transmit antennas ${\cal M}.$

the x-coordinate range of 0 to 5ς and the y-coordinate range of 0 to ς . In **Q-learning**, **MADQN-LR**, and **MADQN**, we employ Q-learning [16], Multi-agent DQN [17] with global reward, and Multi-agent DQN utilizing local rewards for each agent, respectively. Within [10,50] m, we observe an increased performance owing to the reduced channel correlation of the STAR-RISs and the shorter distance between STAR-RISs and users. However, performance declines when the distance ς extends from 50 to 200 m due to dominant high pathloss.

In Fig. 7, we compare the proposed MAGAR algorithm with several benchmarks with different numbers of BS transmit antennas M, cosidering $T_{\rm q}=20,\,V=2,\,N=16,\,K=10,$ and $\varsigma=10.$ We observe that MADQN-LR with local rewards outperforms MADQN using global rewards with around 3%. The proposed MAGAR algorithm, incorporating the global agent, exhibits a significant enhancement in energy efficiency with 7%. As for Q-learning, higher number of BS transmit antennas leads to little improvement of energy efficiency diminishes, as it lacks the neural networks to handle a comparatively large action space under complex environments.

V. CONCLUSION

In this paper, we have conceived an multi-hop STAR-RISassisted transmissions, aiming for maximizing the energy efficiency. We develop a MAGAR algorithm to jointly optimize the active BS beamforming and configurations of STAR-RISs considering the on-off state of STAR-RIS elements. Simulations have demonstrated the effectiveness of the proposed MAGAR scheme in terms of different numbers of STAR-RISs, STAR-RIS elements, transmit antennas, and users. Furthermore, benefited from global agent enhancing collaboration of local agents, our proposed MAGAR algorithm achieves the highest energy efficiency compared to other existing benchmarks.

REFERENCES

- [1] L.-H. Shen, K.-T. Feng, and L. Hanzo, "Five Facets of 6G: Research Challenges and Opportunities," *ACM Computing Surveys*, vol. 55, no. 11, pp. 1–39, 2023.
- [2] L.-H. Shen, K.-T. Feng, T.-S. Lee, Y.-C. Lin, S.-C. Lin, C.-C. Chang, and S.-F. Chang, "AI-Enabled Unmanned Vehicle-Assisted Reconfigurable Intelligent Surfaces: Deployment, Prototyping, Experiments, and Opportunities," *IEEE Network*, pp. 1–1, 2024.
- [3] L.-H. Shen, C.-J. Ku, and K.-T. Feng, "Downlink Rate Maximization with Reconfigurable Intelligent Surface Assisted Full-Duplex Transmissions," *IEEE Transactions on Vehicular Technology*, pp. 1–6, 2024.
- [4] C.-J. Ku, L.-H. Shen, and K.-T. Feng, "Reconfigurable Intelligent Surface Assisted Interference Mitigation for 6G Full-Duplex MIMO Communication Systems," in 2022 IEEE 33rd Annual International Symposium on Personal, Indoor and Mobile Radio Communications (PIMRC), 2022, pp. 327–332.
- [5] F. Fang, B. Wu, S. Fu, Z. Ding et al., "Energy-Efficient Design of STAR-RIS Aided MIMO-NOMA Networks," *IEEE Transactions on Communi*cations, vol. 71, no. 1, pp. 498–511, 2023.
- [6] C. Wu, C. You, S. Han, and M. D. Renzo, "Two-Timescale Design for STAR-RIS-Aided NOMA Systems," *IEEE Transactions on Communica*tions, vol. 72, no. 1, pp. 585–600, 2024.
- [7] C. Huang, G. Chen, J. Tang, Xiao et al., "Machine-Learning-Empowered Passive Beamforming and Routing Design for Multi-RIS-Assisted Multihop Networks," *IEEE Internet of Things Journal*, vol. 9, no. 24, pp. 25 673–25 684, 2022.
- [8] C. Huang, Z. Yang, G. C. Alexandropoulos, Xiong et al., "Multi-Hop RIS-Empowered Terahertz Communications: A DRL-Based Hybrid Beamforming Design," *IEEE Journal on Selected Areas in Communications*, vol. 39, no. 6, pp. 1663–1677, 2021.
- [9] F. D. Tilahun, A. T. Abebe, and C. G. Kang, "DRL-based Distributed Resource Allocation for Edge Computing in Cell-Free Massive MIMO Network," in *Proc. IEEE Global Commun. Conf. (GLOBECOM)*, 2022, pp. 3845–3850.
- [10] H. Zhang, S. Liu, R. Liu, Li et al., "Distributed DRL Based Beamforming Design for RIS-Assisted Multi-Cell Systems," in Proc. IEEE Global Commun. Conf. (GLOBECOM), 2023, pp. 4829–4834.
- [11] S. Pala, M. Katwe, K. Singh, Tsiftsis et al., "Robust Design of RIS-aided Full-Duplex RSMA System for V2X communication: A DRL Approach," in Proc. IEEE Global Commun. Conf. (GLOBECOM), 2023, pp. 2420– 2425.
- [12] Y. Liu, X. Mu, R. Schober, Poor et al., "Simultaneously Transmitting and Reflecting (STAR)-RISs: A Coupled Phase-Shift Model," in Proc. IEEE Int. Conf. Commun. (ICC), 2022, pp. 2840–2845.
- [13] J. Xu, Y. Liu, X. Mu et al., "STAR-RISS: A Correlated T&R Phase-Shift Model and Practical Phase-Shift Configuration Strategies," *IEEE Journal* of Selected Topics in Signal Processing, vol. 16, no. 5, pp. 1097–1111, 2022
- [14] 3rd Generation Partnership Project. (2022, Apr.) Study on channel model for frequencies from 0.5 to 100 GHz (3GPP TR 38.901 version 17.0.0 Release 17). [Online]. Available: www.3gpp.org/DynaReport/38901.htm.
- [15] P. Sunehag, G. Lever, A. Gruslys, W. M. Czarnecki et al., "Value-Decomposition Networks For Cooperative Multi-Agent Learning Based On Team Reward," in Proc. International Foundation for Autonomous Agents and MultiAgent Systems, 2018, p. 2085–2087.
- [16] A. Dridi, C. Boucetta, H. Moungla et al., "Deep Recurrent Learning versus Q-Learning for Energy Management Systems in Next Generation Network," in Proc. IEEE Global Commun. Conf. (GLOBECOM), 2021, pp. 1–6.
- [17] K. Nagarajan and Z. Yi, "Lane Changing Using Multi-Agent DQN," in Proc. IEEE International Conference on Autonomous Systems (ICAS), 2021, pp. 1–6.